ACS Catalysis

Research Article

pubs.acs.org/acscatalysis

Highly Robust Hydrogen Generation by Bioinspired Ir Complexes for Dehydrogenation of Formic Acid in Water: Experimental and Theoretical Mechanistic Investigations at Different pH

Wan-Hui Wang,[†] Mehmed Z. Ertem,[‡] Shaoan Xu,[§] Naoya Onishi,[§] Yuichi Manaka,[§,∥] Yuki Suna,[§] Hide Kambayashi,[§] James T. Muckerman,[*,‡] Etsuko Fujita,[*,‡] and Yuichiro Himeda[*,§,∥]

[†]School of Petroleum and Chemical Engineering, Dalian University of Technology, Panjin 124221, China

[‡]Chemistry Department, Brookhaven National Laboratory, Upton, New York 11973, United States

[§]National Institute of Advanced Industrial Science and Technology, Tsukuba Central 5-1, 1-1-1 Higashi, Tsukuba, Ibaraki 305-8565 Japan

[∥]Japan Science and Technology Agency, CREST, 4-1-8 Honcho, Kawaguchi, Saitama, 332-0012 Japan

Supporting Information

ABSTRACT: Hydrogen generation from formic acid (FA), one of the most promising hydrogen storage materials, has attracted much attention due to the demand for the development of renewable energy carriers. Catalytic dehydrogenation of FA in an efficient and green manner remains challenging. Here, we report a series of bioinspired Ir complexes for highly robust and selective hydrogen production from FA in aqueous solutions without organic solvents or additives. One of these complexes bearing an imidazoline moiety (complex **6**) achieved a turnover frequency (TOF) of 322 000 h^{-1} at 100 °C, which is higher than ever reported. The novel catalysts are very stable and applicable in highly concentrated FA. For instance, complex **3** (1 μmol) affords an unprecedented turnover number (TON) of 2 050 000 at 60 °C. Deuterium kinetic isotope effect experiments and density functional theory (DFT) calculations employing a "speciation" approach demonstrated a change in the rate-determining step with increasing solution pH. This study provides not only more insight into the mechanism of dehydrogenation of FA but also offers a new principle for the design of effective homogeneous organometallic catalysts for H_2 generation from FA.

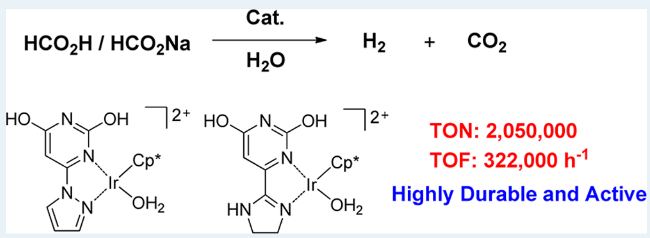

KEYWORDS: *formic acid dehydrogenation, Ir complexes, mechanism, kinetic isotope effect, pH dependence*

INTRODUCTION

A hydrogen economy is a promising alternative to the hydrocarbon economy for solving increasingly severe energy and environmental problems.[1,2] Efficient hydrogen storage is one of the bottlenecks for developing a hydrogen economy.[3−5] Recently, hydrogen storage using formic acid (FA) as a carrier has attracted much attention because of its favorable properties.[6−9] While FA has a relatively low hydrogen content of 4.4 wt %, it is nontoxic, biodegradable, and environmentally friendly. More importantly, it is a liquid under ambient conditions, which makes it easy to store, transport, and handle. FA can be selectively generated by catalytic hydrogenation of CO_2 with a suitable catalyst under mild conditions and can also be used in fuel cells directly. Moreover, FA dehydrogenation can selectively release pressurized H_2/CO_2 with an appropriate catalyst. In some cases, the hydrogen storage capability (i.e., reversible interconversion between CO_2 and FA) can be achieved using the same catalyst by changing reaction conditions such as pressure, temperature, and pH.[10−17]

Various heterogeneous and homogeneous catalysts for FA dehydrogenation have been reported.[6−8,18] Despite recent important progress,[19−22] heterogeneous catalysts often suffer from low activity and selectivity (including the generation of CO that poisons fuel cell catalysts).[8,19] Homogeneous catalysts are generally more effective and attractive[10,23−29] but are far from practical use owing to their limited catalytic efficiency and robustness. The design of highly efficient and robust homogeneous catalysts remains a significant challenge. Nature uses hydrogenase enzymes to accomplish reversible H_2 oxidation (i.e., H_2 splitting and generation, Scheme 1a). An important synergistic effect between the metal center and cooperating ligands in hydrogenases has inspired many chemists to explore such a catalyst design principle (Scheme 1b).[30−33] DuBois et al. have developed a series of complexes with a pendent amine mimicking the structure of [FeFe]-hydrogenase to catalyze various transformations.[34−36] Pincer complexes with noninnocent ligands have also shown outstanding catalytic activity in FA dehydrogenation in organic

Received: February 21, 2015
Revised: July 8, 2015
Published: July 30, 2015

DOI: 10.1021/acscatal.5b01090
ACS Catal. 2015, 5, 5496−5504

Scheme 1. Bioinspired catalyst design for H_2 splitting and generation: (a) The H_2 splitting and generation processes catalyzed by [FeFe]-hydrogenase. (b) Catalyst design with cooperating ligand bearing functional groups for H_2 activation and generation by mimicking the enzyme. (c) Structure of the guanylyl pyridinol (FeGP) cofactor in [Fe]-hydrogenase (GMP: guanidine monophospate). (d) H_2 splitting and generation with our complexes via a synergistic effect between the metal center and cooperating ligands

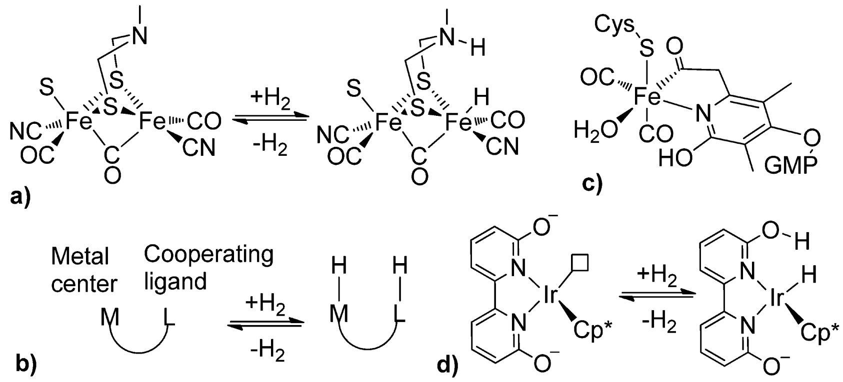

solvents.[10,28,37] Inspired by the active center of [Fe]-hydrogenase (Scheme 1c),[38,39] we have designed and synthesized a series of proton-responsive complexes (Scheme 1d) for efficient catalytic interconversion of formic acid/formate and H_2/CO_2 in water.[14,40−42] The bipyridine or bipyrimidine ligands bearing pendent OH groups are redox noninnocent, and proton-responsive and act as cooperating ligands which have been demonstrated to be largely responsible for the high activity of the complexes.[43] Moreover, the proton-responsive complexes bearing functional OH groups showed tunable activity and can control the equilibrium between formic acid/formate and H_2/CO_2 under different pH conditions. Under acidic conditions, they decompose FA to release H_2/CO_2, while under basic conditions they catalyze CO_2 hydrogenation to provide formate. This unique property is mainly attributed to the pH switchable OH substituent which deprotonates to give the strongly electron-donating oxyanion and improves the activity. Therefore, determination of the exact species in aqueous solution under different pH is highly desirable.

Although various homogeneous catalysts with precious metals or earth-abundant metals have been developed for FA dehydrogenation, high performance (i.e., high TON and TOF) catalysts usually require the presence of organic solvents or additives.[10,27,28,44] Catalysts based on earth-abundant metals typically suffer from low selectivity, and CO contamination is usually observed.[26,28,45] The presence of the amine in an FA/amine system results in a loss of the volatile amine. In contrast, FA dehydrogenation in water without organic additives is eco-friendly, and a highly concentrated FA solution can also provide good hydrogen capacity. However, reports of highly active and stable catalysts in aqueous solution are scarce.[16,46−48] We recently reported that a five-membered azole moiety is an efficient electron donor, and its incorporation into a catalyst complex is effective for FA dehydrogenation in water.[49] This is supposedly due to the high electron donating ability of the azole moieties. Taking into account that pyridine and pyrimidine ligands bearing pendent OH groups are effective for H_2 activation, we focused on designing new catalysts that combine pyridine or pyrimidine moieties bearing pendent OH groups with electron-donating azole and azoline moieties including pyrazole, imidazole, and imidazoline. Herein, we report unprecedentedly durable bioinspired complexes for catalyzing FA dehydrogenation in water (TON of 2 050 000 at 60 °C). Furthermore, an initial TOF as high as 332 000 h^{-1} could be achieved in 4 M HCO_2H/HCO_2Na (68/32) using a complex based on an imidazoline ligand.

The deuterium kinetic isotope effect (KIE) is an effective method for exploring reaction mechanisms.[10,50−52] We have previously investigated the mechanism of formic acid dehydrogenation with KIE studies[50] and demonstrated a significant effect depending on the specific ligands with or without pendent OHs in the complexes. Complexes with 6,6′-dihydroxy-2,2′-bipyridine (OH substituents in *ortho* positions) exhibit a different pH dependence than those with 4,4′-dihydroxy-2,2′-bipyridine (OH substituents in *para* positions) owing to the two classes of complexes having different rate-determining steps (RDS) in the catalytic cycle.[41] Dehydrogenation of formic acid is known to exhibit a pH dependence, which suggests that the solution pH has an important influence on the reaction rate;[14,52−54] however, to the best of our knowledge, the effect of solution pH on the mechanism has not yet been comprehensively studied. Here, we demonstrate for the first time that the rate-determining step for a catalyst that has a 6,6′-dihydroxy-2,2′-bipyridine-like ligand (OH substituent in an *ortho* position) changes upon altering the solution pH, and we rationalize the bell-shaped pH dependence of the activity of such catalysts through a combined experimental and computational effort. In the calculations, we employ a "speciation" approach which helps to determine the actual species (i.e., fully deprotonated or partially deprotonated) in the reaction solution.

■ RESULTS AND DISCUSSION

Catalyst Screening. The water-soluble complexes **1**−**6** (Chart 1) were synthesized using methods similar to those previously reported (see SI).[42,43] With these complexes in hand, we carried out the catalytic dehydrogenation of formic acid in aqueous solutions at low FA concentration (1 M) and temperature (60 °C, Table 1). Complex **1** bearing a MeO group showed moderate activity (TOF: 1010 h^{-1}, entry 1) in 1 M HCO_2H solution (pH 1.7) and apparent decreased activity (TOF: 160 h^{-1}, entry 2) in 1 M HCO_2H/HCO_2Na (1/1, pH 3.5). In contrast, complex **2** with a pendent OH group showed significant improvement in activity and stability (entries 3 and 4). The TOF increased to 2740 h^{-1} in 1 M HCO_2H and further increased to 3620 h^{-1} in 1 M HCO_2H/HCO_2Na (1/1, pH 3.5).

DOI: 10.1021/acscatal.5b01090
ACS Catal. 2015, 5, 5496−5504

Chart 1. Novel Biomimetic Complexes for FA Dehydrogenation in Aqueous Solution

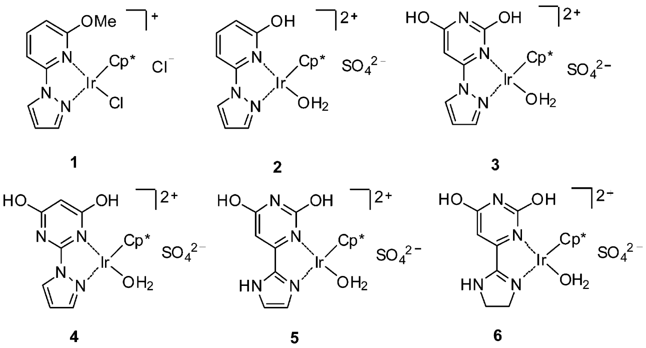

Table 1. Dehydrogenation of FA with Ir Complexes 1−6[a]

entry	catalyst, μM	solution pH	time, h	TON	TOF[b] h^{-1}
1	**1**, 100	1.7	5	2570	1010
2	**1**, 100	3.5	5	430	160
3	**2**, 100	1.7	7	10 000	2740
4	**2**, 100	3.5	7	5000	3620
5	**3**, 100	1.7	7	10 000	7050
6	**3**, 100	3.5	1	5500	11 400
7	**3**, 100	2.8	1.5	8700	18 000
8	**4**, 100	1.7	3.5	10 000	5150
9	**4**, 100	3.0	1.5	7640	10 800
10	**5**, 100	1.7	5	10 000	4290
11	**5**, 100	3.0	1	7850	19 900
12	**6**, 100	1.7	3	10 000	5520
13	**6**, 100	3.0	0.5	7850	32 500

[a]Reaction conditions: 1 M HCO_2H or HCO_2H/HCO_2Na solution (10 mL) with Ir complexes 1 μmol at 60 °C. All numbers are an average of two runs. FA dehydrogenation reactions with complexes **2**−**6** yielded complete FA decomposition. [b]Average TOF over initial 10 min.

These pH dependences are consistent with our previous report that complexes with pendent OH groups in the second coordination sphere exhibit a bell-shaped pH vs rate profile.[41] In 1 M FA solution, complex **3** gave an initial TOF of 7050 h^{-1} at 60 °C (entry 5). The initial TOF in 1 M HCO_2H/HCO_2Na (1/1, pH 3.5) reached 11 400 h^{-1}, which is triple that of complex **2** (entry 6). Similar to all the complexes with pendent OH groups, its pH vs rate profile also was bell-shaped (Figure 1), and the TOF peaked at pH 2.8 (TOF: 18 000 h^{-1}, entry 7). Changing the position of the N in the pyrimidine ring led to a considerable decrease in the activity of the complex as shown in the pH vs rate profile (Figure 1, **3** vs **4**). Complex **4** gave a TOF of 5150 h^{-1} at pH 1.7 and 60 °C (entry 8). The TOF peaked at pH 3.0 (TOF: 10 800 h^{-1}, entry 9). Replacing the pyrazole ring with an imidazole ring led to both low stability and activity at low solution pH. Complex **5** was found to have partially precipitated from the solution at some point during the reaction at pH below 2.6, leading to decreased activity. The TOF at pH 1.7 was 4290 h^{-1}, which is even lower than that of complex **4** (entry 10). Interestingly, the reaction rate increased significantly with increasing solution pH. The maximum TOF value (19 900 h^{-1}, entry 11) at pH 3.0 is even higher than that of complex **3** (Figure 1, **3** vs **5**). When complex **6** bearing an imidazoline ring was used, we observed no apparent catalyst precipitation, but similar to complex **5** the reaction rate increased significantly with increasing solution pH (Figure 1, **6**). It exhibited the highest initial TOF of 32 500 h^{-1} at pH 3.0 (entry 13). The catalytic efficiency of complex **6** is even higher than the most efficient Ir dinuclear complex with 4,4′,6,6′-tetrahydroxy-2,2′-pyrimidine under similar conditions.[14]

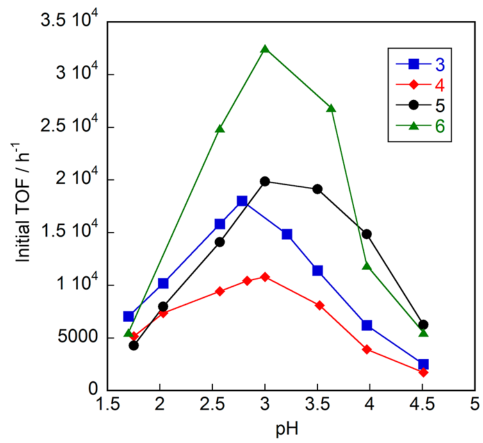

Figure 1. pH dependence of FA dehydrogenation using complexes **3**−**6** (100 μM) in 1 M HCO_2H/HCO_2Na (10 mL) solution at 60 °C.

Durability Tests. For practical use in FA dehydrogenation, a high concentration of FA and a high temperature are required. Therefore, we carried out FA dehydrogenation under harsher conditions with complexes **3**−**6** that showed remarkable activity in the preliminary experiments. The experiments examining the temperature dependence with complex **3** suggested that the reaction rate increased significantly upon increasing the reaction temperature from 45 to 70 °C (SI, Figure S1). The FA concentration was also found to be an important factor for the increase in the reaction rate. The reaction rate reached a maximum in 4 M FA solution using either complex **3** or **4** (SI, Figures S2 and S4). In addition, the capability of generating high pressure gases is desirable for the convenience of gas delivery. We carried out the FA dehydrogenation with complex **3** in a closed system. The inner pressure of the autoclave reached a final pressure of 4 MPa after the reaction completed (SI, Figure S5). According to the HPLC analysis, 99.4% of the FA was converted. This is consistent with our previous reports[14,49] and suggests that high pressure does not inhibit the catalytic activity of complex **3**. Therefore, under acidic conditions, the equilibrium between CO_2/H_2 and HCO_2H of this catalytic system is strongly biased toward gas generation, and pressure only weakly affects the equilibrium. Moreover, no CO was detected by GC (detection limit 1 ppm) from the released gas. This indicates that the catalytic reaction is highly selective and goes through no dehydration, which generates CO and H_2O. These properties are important for providing high pressure H_2 which facilitates gas delivery and utilization in fuel cells because CO is a poison for the catalyst in fuel cell electrodes.

Complexes **3** and **4** were found to be stable in highly concentrated FA solutions at both low (60 °C, SI, Figure S6) and high (100 °C, SI, Figures S9−S11) temperatures. The reaction results in highly concentrated FA solution, and high temperatures are listed in Table 2. All the FA was completely decomposed at 100 °C (110 °C bath temperature; the actual reaction temperatures measured were close to 100 °C) with only 20 μM catalyst concentration (Table 2, entries 1−4). In contrast, complexes **5** and **6** were relatively less stable under the same conditions. A higher catalyst concentration (100 μM) was

DOI: 10.1021/acscatal.5b01090
ACS Catal. 2015, 5, 5496−5504

Table 2. H_2 Generation from Dehydrogenation of FA at High Concentration and High Temperature with Ir Complexes 3–6[a]

entry	catalyst, μM	conc. and substrate	time, h	TON	TOF[b]/h^{-1}
1	**3**, 20	4 M FA	2	200 000	178 000
2	**3**, 20	6 M FA	3.5	300 000	176 000
3	**3**, 20	8 M FA	4	400 000	173 000
4	**4**, 20	4 M FA	3.5	200 000	120 000
5	**5**, 100	4 M FA	1	40 000	89 400
6	**6**, 100	4 M FA	1.5	40 000	68 600
7	**3**, 20	4 M 98/2[d]	6	196 000	269 000
8[c]	**6**, 40	4 M 80/20[d]	5	80 000	258 000
9[c]	**6**, 40	4 M 68/32[d]	0.5	68 000	322 000

[a]Reaction conditions: 0.2–1 μmol Ir complexes in 10 mL of HCO_2H or HCO_2H/HCO_2Na solution at 100 °C (110 °C bath temperature; the actual reaction temperatures measured were close to 100 °C). All numbers are an average of two runs. [b]Average TOF over initial 10 min. [c]50 mL HCO_2H/HCO_2Na solution. [d]The ratio of HCO_2H to HCO_2Na.

required for complete conversion of the FA (entries 5 and 6). Complex **3** showed excellent stability. This complex is quite stable in highly concentrated FA solutions (even 80 wt % FA), and all the FA could be dehydrogenated (TON: 200 000) despite the fact that the TOF decreased considerably (SI, Figure S7). Interestingly, we observed an apparent increase of reaction rate with consumption of FA and a decrease of FA concentration. The rate around 9000 min is higher than that at the initial stage or around 1500 min. This is in agreement with our study of the effect of FA concentration as shown in Figures S2 and S4.

Complex **3** gave the high TOF of 178 000 h^{-1} at 100 °C in 4 M FA (entry 1). The initial reaction rate decreased slightly upon increasing the FA concentration (entries 1–3). The reaction in 8 M FA was finished in 4 h and exhibited the high TON of 400 000 (entry 3). Using complex **4** in 4 M FA at 100 °C, the TOF of 120 000 h^{-1} was slightly lower than that of complex **3** (entry 4 vs entry 1). We obtained relatively lower TOF values with complexes **5** and **6** in 4 M FA (entries 5 and 6). As the pH vs rate profile suggested, the addition of formate can significantly improve the reaction rate. Thus, we tried a 4 M HCO_2H/HCO_2Na (98/2) solution at 100 °C (entry 7). Accordingly, complex **3** achieved a significantly elevated initial TOF of 269 000 h^{-1}. With the same strategy, we optimized the reaction conditions and obtained the unprecedented initial TOF of 322 000 h^{-1} with complex **6** (entry 9), which is higher than for any catalyst previously reported.[10,25,28,55] These results indicate that both complexes **3** and **6** show much higher activity than the most effective dinuclear Ir complex previously reported.[14] These water-soluble complexes in aqueous media are even more efficient than the very recently reported PNP-Ru in DMF/Et_3N for FA dehydrogenation.[10]

Based on the results obtained in these preliminary experiments with highly stable and efficient complex **3**, we sought to maximize its TON for FA dehydrogenation. Unprecedentedly high TONs (more than 2 million) were reproducibly obtained in highly concentrated aqueous FA solutions for long reaction times (Figure 2). Sodium formate was not added to increase the reaction rate because sodium formate cannot be decomposed and decreases the total TON. Considering that the practical use would probably be carried out under milder conditions to achieve a lower energy cost, we carried out the

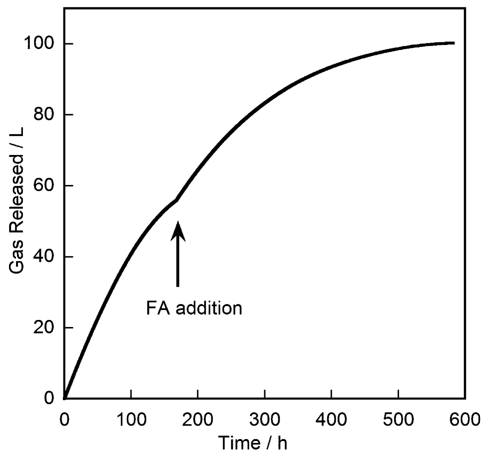

Figure 2. Time course of formic acid dehydrogenation using complex **3** (1 μmol) in a 6 M aqueous FA solution (200 mL, 1.2 mol). Additional FA (50 wt % solution 74 g, ~ 0.8 mol) at 60 °C was added after 167 h. A total of 100.2 L of gas was generated (see SI).

reaction at the relatively lower temperature of 60 °C. The reaction proceeded smoothly using only 1 μmol of catalyst (catalyst concentration: 5 μM) in 200 mL of 6 M FA aqueous solution. After 150 h, the rate of dehydrogenation became slower due to the decrease of FA concentration. After 55 L of gas were released (167 h), a degassed 50 wt % solution of FA (74 g, approximately 0.8 mol FA) was added (see SI). The addition of FA restarted the gas generation and indicated that the catalyst was still active after the first run. Finally, 100.2 L of gas were evolved and afforded the extraordinary TON of 2 050 00, which, to the best of our knowledge, is higher than ever reported for either an aqueous or organic solvent system.

KIE Studies. The proposed mechanism for FA dehydrogenation (Scheme 2) starts with the binding of HCO_2H or

Scheme 2. Change in Rate Determining Step with Altered Solution pH for Complex 3 in FA Dehydrogenation

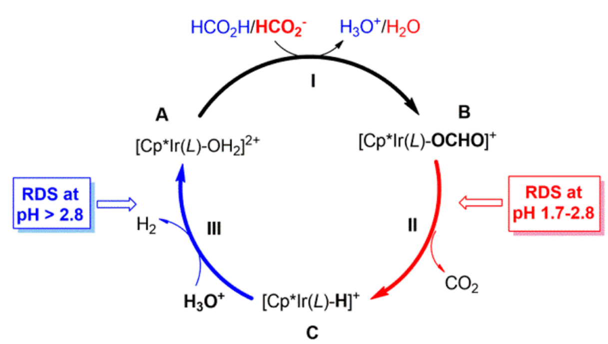

formate, resulting in a formate-bound intermediate **B** (step I). Then, β-hydride elimination with concomitant CO_2 evolution leads to the formation of an Ir-hydride intermediate **C** (step II). Following this step, H_2 is formed via proton transfer from a hydroxy group of the pyrimidine ring of **3** to an Ir-hydride moiety (step III) assisted by a water molecule,[43] completing the catalytic cycle (Schemes 3 and 4).

We have reported different rate-determining steps for complexes with and without pendent OH groups based on deuterium kinetic isotope effect studies.[41] However, the KIE studies were limited to the regime in which the reaction rates were increasing (see Figure 1). The KIE results can explain the

DOI: 10.1021/acscatal.5b01090
ACS Catal. 2015, 5, 5496–5504

Scheme 3. Proposed Mechanism for FA Dehydrogenation by Complex 3 at pH 1.7 and 333.15 K[a]

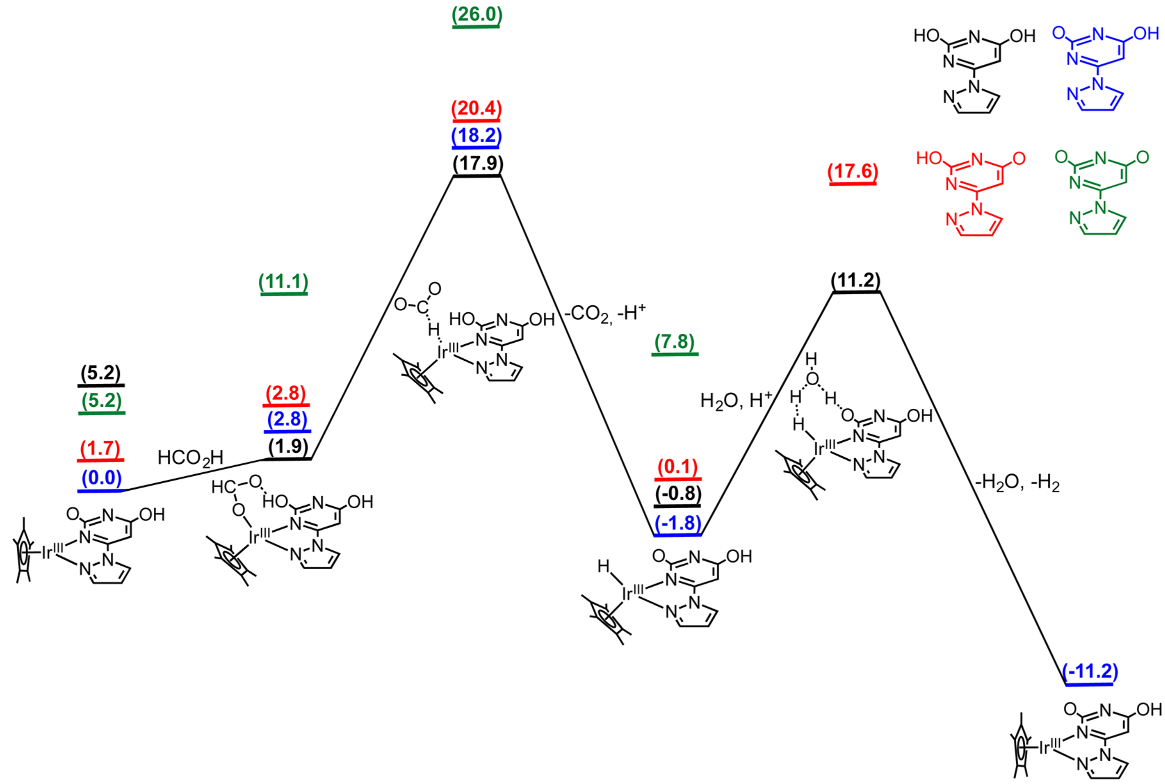

[a]The relative free energies are reported in units of kcal/mol. The speciation of the protonation state of each intermediate and transition state is indicated by the color code of the structures in the upper right of the scheme.

Scheme 4. Proposed Mechanism for FA Dehydrogenation by Complex 3 at pH 3.5 and 333.15 K[a]

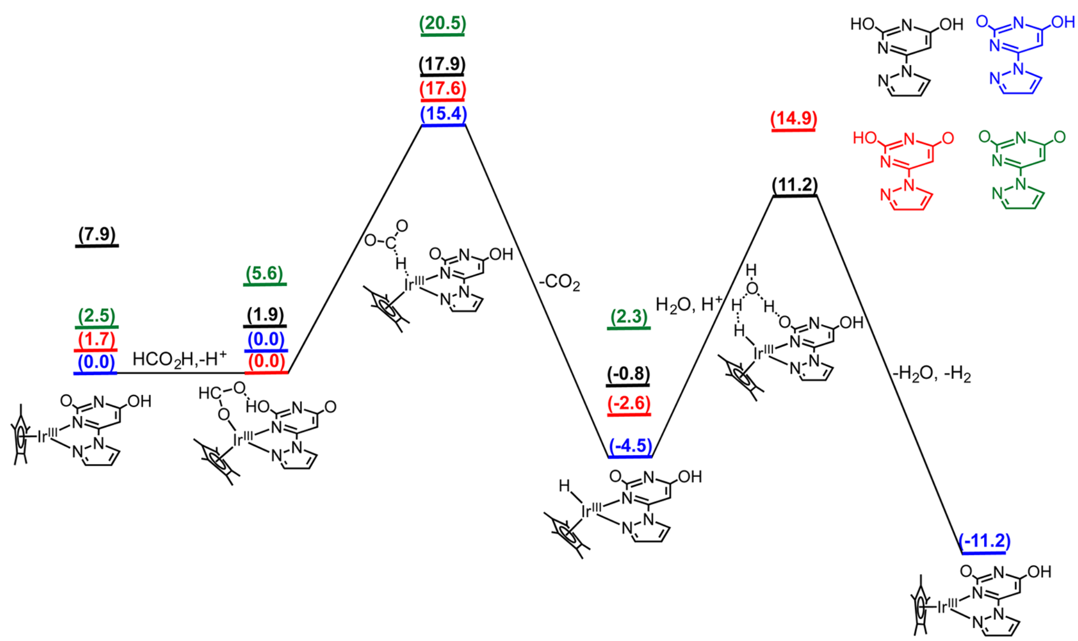

[a]The relative free energies are reported in units of kcal/mol. The speciation of the protonation state of each intermediate and transition state is indicated by the color code of the structures in the upper right of the scheme.

rate increase with increasing solution pH but cannot explain the reaction rate decrease with a further increase of solution pH. The high catalytic activity of these complexes at low pH and high pH above and below the peak motivated further studies of the KIE values at pH values on both sides of the peak of the bell-shaped activity curve. Accordingly, we performed a KIE study with complex **3**, which peaked at pH 2.8 as shown in the pH vs rate profile of Figure 1. The reactions were carried out in 1 M formic acid solution (pH 1.7) and 1 M HCO_2H-HCO_2Na (1/1) solution (pH 3.5), and the results are shown in Table 3.

DOI: 10.1021/acscatal.5b01090
ACS Catal. 2015, 5, 5496−5504

Table 3. Kinetic Isotope Effect in the Dehydrogenation of FA Using Ir Complex 3[a]

entry	substrate/ solvent (pH 1.7)	TOF[b]/ h^{-1}	KIE[c]	substrate/ solvent (pH 3.5)	TOF[b]/ h^{-1}	KIE[c]
1	HCO_2H H_2O	14 000		HCO_2H-HCO_2Na H_2O	16 600	
2	HCO_2H D_2O	9570	1.5	HCO_2H-HCO_2Na D_2O	6130	2.7
3	DCO_2D H_2O	6870	2.0	DCO_2D-DCO_2Na H_2O	11 200	1.5
4	DCO_2D D_2O	4430	3.2	DCO_2D-DCO_2Na D_2O	5090	3.3

[a]Reaction conditions: 10 mL 1 M FA solution or FA/formate (1/1), 1 μmol catalyst, 70 °C. [b]Average TOF over the initial 10 min. The errors are less than 2%. [c]KIE = TOF(entry 1)/TOF(entry *n*), (*n* = 2, 3, and 4). The exchange of all labile protons was taken into account.

Table 4. Kinetic Isotope Effect in the Dehydrogenation of FA Using Ir Complex 6[a]

entry	substrate/ solvent (pH 1.7)	TOF[b] h^{-1}	KIE[c]	substrate/ solvent (pH 3.5)	TOF[b]/ h^{-1}	KIE[c]
1	HCO_2H H_2O	13 300		HCO_2H-HCO_2Na H_2O	28 800	
2	HCO_2H D_2O	9080	1.5	HCO_2H-HCO_2Na D_2O	23 200	1.2
3	DCO_2D H_2O	5770	2.3	DCO_2D-DCO_2Na H_2O	25 300	1.1
4	DCO_2D D_2O	3440	3.9	DCO_2D-DCO_2Na D_2O	18 200	1.6

[a]Reaction conditions: 10 mL 1 M FA solution or FA/formate (1/1), 1 μmol catalyst, 70 °C. [b]Average TOF over the initial 10 min. The errors are less than 2%. [c]KIE = TOF(entry 1)/TOF(entry *n*), (*n* = 2, 3, and 4). The exchange of all labile protons was taken into account.

The KIE study at pH 1.7 suggests that DCO_2D (KIE: 2.0, entry 3) is more influential than D_2O (KIE: 1.5, entry 2) on the reaction rate. Therefore, the *β*-hydride elimination (Scheme 2, step II), which involves Ir−D bond formation when DCO_2D is used, was designated as the rate-determining step. This result is consistent with our previous report[41] and other reports.[26,51,52] The examination of FA concentration as shown in Figures S2 and S4 also supports step II as being rate-limiting around pH 1.7. The rate improvement from 1 to 4 M FA could be explained by considering a pre-equilibrium associated with the formation of a formate bound Ir complex (**B** in Scheme 2) prior to the rate determining *β*-hydride elimination step (see Figure S3 and SI for details). Since formation of **B** requires deprotonation, decreasing the pH with increased FA concentration will slow down the reaction. On the other hand, increasing concentration of one of the reactants (e.g., HCO_2H) will favor formation of **B**, hence the net outcome of increasing FA concentration will be determined by these two countereffects. Using a simple rate expression for the *β*-hydride elimination step including the pre-equilibrium for the formation of **B** indicates that the rate will be enhanced by 1.6 times upon changing the FA concentration from 1 to 4 M, which is in good agreement with the experimental observation (Figure S2). A further increase in FA concentration will slow down the deprotonation step for the formation of **B** to a greater extent and will result in a decrease in the overall reaction rate.

When a KIE study was carried out at pH 3.5 using HCO_2H-HCO_2Na in the ratio of 1:1, the results were surprising. The KIE value (2.7) using D_2O is higher than that (1.5) using DCO_2D-DCO_2Na (entry 2 vs entry 3), suggesting that H_2O or H_3O^+ is involved in the rate-determining step. Therefore, as shown in Scheme 2, the RDS should be H_2 formation (step III) when pH > 2.8. Based on these results, we propose that the rate-determining step is *β*-hydride elimination (Scheme 2, step II) at pH 1.7−2.8 and changes to H_2 formation (Scheme 2, step III) when pH > 2.8 (see Computational Studies below). We carried out a similar KIE study with complex **6** (Table 4). Similarly, deuterated solvent showed much greater influence than the deuterated substrate upon changing solution pH from 1.7 to 3.5. These results are consistent with those of complex **3** and indicate the altering of the RDS. The interesting RDS change is attributed to the loss or gain of one or more protons by the intermediate along the reaction pathway,[56] therefore a detailed computational investigation of the actual forms of the intermediates of the proton responsive catalysts was performed using DFT calculations.

Computational Studies. We performed density functional theory (DFT) calculations at the M06 level of theory[57] with the SMD aqueous continuum solvation model[58] (see Computational Methods in the SI for details) to investigate the mechanistic details associated with FA dehydrogenation by complexes **2**, **3**, **5**, and **6**. We have demonstrated that the proton-responsive complexes containing a proximal $-O^-$ group can facilitate the hydrogen splitting through hydrogen bonding (Scheme 1d).[43] Thus, in the reverse reaction, the proximal $-O^-$ can also assist the hydrogen formation. A sulfonamide ligand-assisted FA dehydrogenation via hydrogen bonding has been reported.[59] Further considering the different hydrogen bonding model and different electron donating ability between $-OH$ and $-O^-$, it is highly desirable to determine the real forms of the proton-responsive complexes in the solution at different pH, i.e., the protonated form or a fully or partially deprotonated form. Therefore, we applied a speciation approach in which we calculated the relative free energies of the intermediates and transition-state structures for all possible protonation states of the complexes and followed the changes in relative free energies with changes in pH. For instance, for FA dehydrogenation by **3**, we generated free-energy profiles at pH 1.7 and 3.5 following the relative free energies of intermediates and transition state structures differing in protonation states as depicted in Schemes 3 and 4. Similar free-energy plots for complexes **2**, **5**, and **6** are presented in the SI (Schemes S1−S19).

For the following energetic analysis of the proposed catalytic cycle, we have used the free energies associated with the most stable species for each reaction intermediate as shown in Schemes 3 and 4 connected by a black solid line. The reasoning behind this convention (or "speciation" approach) is that deprotonation of an OH group will be more facile than traversing a transition state for *β*-hydride elimination or H_2 formation so that the most stable protonation state of each species will be predominant in the solution. At pH 1.7, the binding of formic acid is uphill by 1.9 kcal/mol, and the following *β*-hydride elimination step features a free energy of activation ($\Delta G^‡$) of 16.0 kcal/mol (Scheme 3). H_2 formation from the generated Ir-hydride species occurs with $\Delta G^‡$ = 13.0

DOI: 10.1021/acscatal.5b01090
ACS Catal. 2015, 5, 5496−5504

kcal/mol, releasing $H_{2(g)}$ and regenerating the catalyst (Scheme 3). At pH 3.5, the formation of the formate complex requires no energy input (ΔG = 0.0 kcal/mol), and the $\Delta G^{\ddagger}$ for the following β-hydride elimination step is 15.4 kcal/mol (Scheme 4). The following H_2 formation step involves a $\Delta G^{\ddagger}$ of 15.7 kcal/mol at pH 3.5 (Scheme 4). The calculated $\Delta G^{\ddagger}$ values are 16.0 and 13.0 kcal/mol at pH 1.7 corresponding to the β-hydride elimination and H_2 generation steps, respectively, indicating that the former is the rate-determining step (Scheme 3). The calculated overall energy barrier for the β-hydride elimination step (17.9 kcal/mol) including the free-energy cost for HCO_2H binding is consistent with the experimental observation of an activation energy of 18.7 kcal/mol (SI, Figure S1).

On the other hand, at pH 3.5, $\Delta G^{\ddagger}$ = 15.4 kcal/mol for β-hydride elimination and $\Delta G^{\ddagger}$ = 15.7 kcal/mol for H_2 generation, indicating that the latter is becoming the rate-determining step as the pH is increased (Scheme 4). Based on these data, the β-hydride elimination is the rate-determining step at low pH, but the free-energy cost for H_2 generation increases with increasing pH. The catalyst displays the highest rate at moderate pH when the $\Delta G^{\ddagger}$ values of the two steps are very close, consistent with the experimental observation of the bell shaped pH vs rate profile (Figure 1) and the H_2 generation step becoming rate-determining with a further increase in pH as suggested by the KIE experiments. It should be kept in mind that the difference in the $\Delta G^{\ddagger}$ values at pH 3.5 is probably within the error in both the calculated and experimental values, but the trend from pH 1.7 should be more reliable.

We also calculated KIEs for the β-hydride elimination and H_2 generation steps for complex **3** associated with deuterium substitution either on the substrate or on the solvent (Table 5).

Table 5. Calculated Kinetic Isotope Effects for β-Hydride Elimination and H_2 Generation Steps for Complex 3 at T = 343.15 K

substrate/solvent	β-hydride elimination	H_2 generation[a]
HCO_2H/D_2O	1.0	4.7
DCO_2D/H_2O	2.4	1.0
DCO_2D/D_2O	2.4	4.5

[a]The reactant complex, similar to the transition state, involves additional explicit water for KIE calculations. The exchange of all labile protons was taken into account.

It is clear from the calculated KIEs that β-hydride elimination is mostly affected by deuteration of formic acid, and the H_2 generation step is more affected by the deuteration of water. The experimentally observed dependence of KIEs on pH, taken together with the calculated KIEs, further support the notion of a change in the rate-determining step from β-hydride elimination to H_2 generation with increasing pH, and at pH 3.5 is approaching the value at which that change will occur.

The calculated $\Delta G^{\ddagger}$ values for the β-hydride elimination and H_2 generation steps at different pH for complexes **2**, **3**, **5**, and **6** provide some insight for the design of improved catalysts for FA dehydrogenation (Table 6). Comparison of $\Delta G^{\ddagger}$ values of the rate-determining steps at pH 1.7 and 3.5 for complexes **2** and **3** indicates that the substitution of the hydroxy pyridine ligand in **2** with the dihydroxy pyrimidine ring in **3** decreases the free energies of activation, consistent with the experimentally observed enhanced activity of **3**. For complexes **2** and **3**, the $\Delta G^{\ddagger}$ values clearly indicate the change of RDS from β-hydride elimination to H_2 generation with increasing pH from 1.7 to 3.5. Although the $\Delta G^{\ddagger}$ values of complexes **5** and **6** showed no switching of RDS at 333.15 K, the $\Delta G^{\ddagger}$'s for the H_2 generation step are becoming larger, and the difference between the two steps is becoming smaller. From this viewpoint, this tendency also supports the change of RDS with increasing solution pH. From the results of our calculations, we expect the switchover point for complexes **5** and **6** to be larger than the experimental observation (pH 3.1), which could be attributed to the associated errors in the DFT calculation. We also calculated the free energies of activation at 373.15 K for complexes **3** and **6**. At this temperature, the H_2 formation step becomes the rate-determining step for both complex **3** ($\Delta G^{\ddagger}$ = 17.6 kcal/mol) and complex **6** ($\Delta G^{\ddagger}$ = 20.0 kcal/mol) with the former showing the highest activity at pH 2.8 and the latter showing enhanced activity at the slightly elevated pH of 3.1 (SI, Schemes S1−S19).

Table 6. Calculated Free Energies of Activation ($\Delta G^{\ddagger}$) Associated with Relevant TSs for β-Hydride Elimination and H_2 Generation Steps for Complexes 2, 3, 5, and 6 at T = 333.15 K for Different pH Values

		free energies of activation (kcal/mol) associated with relevant TSs			
		complex **2**	complex **3**	complex **5**	complex **6**
pH 1.7	β-hydride elimination	17.2	16.0	18.1	18.4
	H_2 generation	15.7	13.0	12.9	13.6
pH 3.5	β-hydride elimination	15.9	15.4	16.7	17.6
	H_2 generation	16.1	15.7	14.8	16.4

■ CONCLUSIONS

We have designed and synthesized a series of biomimetic Ir complexes with hydroxy substituted pyridine-azole and pyrimidine-azole/azoline ligands. These water-soluble complexes are demonstrated to be highly efficient and stable in catalytic FA dehydrogenation at high temperature in highly concentrated FA aqueous solutions. We have achieved the unprecedented TOF of 322 000 h^{-1} and TON of 2 050 000 with the most effective complexes **6** and **3**, respectively. These complexes are capable of providing high pressure CO-free H_2. The extraordinary catalytic performance indicates that these complexes should be highly useful in the practical supply of H_2 from FA and contributes significantly to the development of a hydrogen economy. Investigation of the mechanism using deuterium KIE studies and DFT calculations suggests that the rate-determining steps are altered upon changing the solution pH. The DFT calculations employing a "speciation" approach provide insight into the mechanism and support the RDS change. This mechanistic insight rationalizes the bell-shaped pH vs rate profile and helps to determine the optimal conditions of FA dehydrogenation by the addition of formate and adjustment of the solution pH.

■ ASSOCIATED CONTENT

Ⓢ Supporting Information

The Supporting Information is available free of charge on the ACS Publications website at DOI: 10.1021/acscatal.5b01090.

Experimental section containing general procedures and synthesis of ligands and Ir complexes, a plot of TOF vs temperature for FA dehydrogenation, plots of FA

DOI: 10.1021/acscatal.5b01090
ACS Catal. 2015, 5, 5496−5504

dehydrogenation, TOF vs [HCO_2H], plots of time courses of FA decomposition, computational methods, free-energy profiles derived from DFT calculations for FA dehydrogenation for complexes **2**−**6** at pH 1.7 and 3.5, tables of optimized coordinates and energies, and ^1H NMR spectra of ligands (PDF)

AUTHOR INFORMATION

Corresponding Authors

*E-mail: muckerma@bnl.gov.
*E-mail: fujita@bnl.gov.
*E-mail: himeda.y@aist.go.jp.

Notes

The authors declare no competing financial interest.

ACKNOWLEDGMENTS

Y.H. and Y.M. thank the Japan Science and Technology Agency (JST), CREST for financial support. W.-H.W. is thankful for the financial support from Dalian University of Technology (the Fundamental Research Funds for the Central Universities, Grant No. DUT14RC(3)082; Grant No. 844401) and National Natural Science Foundation of China (Grant No. 21402019). The work at BNL was carried out under contract DE-SC00112704 with the U.S. Department of Energy, Office of Science, Office of Basic Energy Sciences, and utilized resources at the BNL Center for Functional Nanomaterials.

REFERENCES

(1) Züttel, A.; Borgschulte, A.; Schlapbach, L. *Hydrogen as a future energy carrier*; Wiley-VCH: Weinheim, 2008; pp 1−6.
(2) Armaroli, N.; Balzani, V. *ChemSusChem* **2011**, *4*, 21−36.
(3) Makowski, P.; Thomas, A.; Kuhn, P.; Goettmann, F. *Energy Environ. Sci.* **2009**, *2*, 480−490.
(4) Eberle, U.; Felderhoff, M.; Schüth, F. *Angew. Chem., Int. Ed.* **2009**, *48*, 6608−6630.
(5) Yadav, M.; Xu, Q. *Energy Environ. Sci.* **2012**, *5*, 9698−9725.
(6) Johnson, T. C.; Morris, D. J.; Wills, M. *Chem. Soc. Rev.* **2010**, *39*, 81−88.
(7) Enthaler, S.; von Langermann, J.; Schmidt, T. *Energy Environ. Sci.* **2010**, *3*, 1207−1217.
(8) Grasemann, M.; Laurenczy, G. *Energy Environ. Sci.* **2012**, *5*, 8171−8181.
(9) Joó, F. *ChemSusChem* **2008**, *1*, 805−808.
(10) Filonenko, G. A.; van Putten, R.; Schulpen, E. N.; Hensen, E. J. M.; Pidko, E. A. *ChemCatChem* **2014**, *6*, 1526−1530.
(11) Boddien, A.; Federsel, C.; Sponholz, P.; Mellmann, D.; Jackstell, R.; Junge, H.; Laurenczy, G.; Beller, M. *Energy Environ. Sci.* **2012**, *5*, 8907−8911.
(12) Preti, D.; Squarcialupi, S.; Fachinetti, G. *Angew. Chem., Int. Ed.* **2010**, *49*, 2581−2584.
(13) Maenaka, Y.; Suenobu, T.; Fukuzumi, S. *Energy Environ. Sci.* **2012**, *5*, 7360−7367.
(14) Hull, J. F.; Himeda, Y.; Wang, W.-H.; Hashiguchi, B.; Periana, R.; Szalda, D. J.; Muckerman, J. T.; Fujita, E. *Nat. Chem.* **2012**, *4*, 383−388.
(15) Boddien, A.; Gartner, F.; Federsel, C.; Sponholz, P.; Mellmann, D.; Jackstell, R.; Junge, H.; Beller, M. *Angew. Chem., Int. Ed.* **2011**, *50*, 6411−6414.
(16) Papp, G.; Csorba, J.; Laurenczy, G.; Joó, F. *Angew. Chem., Int. Ed.* **2011**, *50*, 10433−10435.
(17) Hsu, S.-F.; Rommel, S.; Eversfield, P.; Muller, K.; Klemm, E.; Thiel, W. R.; Plietker, B. *Angew. Chem., Int. Ed.* **2014**, *53*, 7074−7078.
(18) Loges, B.; Boddien, A.; Gartner, F.; Junge, H.; Beller, M. *Top. Catal.* **2010**, *53*, 902−914.
(19) Bulushev, D. A.; Beloshapkin, S.; Ross, J. R. H. *Catal. Today* **2010**, *154*, 7−12.
(20) Bavykina, A. V.; Goesten, M. G.; Kapteijn, F.; Makkee, M.; Gascon, J. *ChemSusChem* **2015**, *8*, 809−812.
(21) Bi, Q. Y.; Lin, J. D.; Liu, Y. M.; Du, X. L.; Wang, J. Q.; He, H. Y.; Cao, Y. *Angew. Chem., Int. Ed.* **2014**, *53*, 13583−13587.
(22) Chen, Y.; Zhu, Q.-L.; Tsumori, N.; Xu, Q. *J. Am. Chem. Soc.* **2015**, *137*, 106−109.
(23) Fellay, C.; Dyson, P. J.; Laurenczy, G. *Angew. Chem., Int. Ed.* **2008**, *47*, 3966−3968.
(24) Loges, B.; Boddien, A.; Junge, H.; Beller, M. *Angew. Chem., Int. Ed.* **2008**, *47*, 3962−3965.
(25) Barnard, J. H.; Wang, C.; Berry, N. G.; Xiao, J. *Chem. Sci.* **2013**, *4*, 1234−1244.
(26) Boddien, A.; Mellmann, D.; Gartner, F.; Jackstell, R.; Junge, H.; Dyson, P. J.; Laurenczy, G.; Ludwig, R.; Beller, M. *Science* **2011**, *333*, 1733−1736.
(27) Zell, T.; Butschke, B.; Ben-David, Y.; Milstein, D. *Chem. - Eur. J.* **2013**, *19*, 8068−8072.
(28) Bielinski, E. A.; Lagaditis, P. O.; Zhang, Y.; Mercado, B. Q.; Wuertele, C.; Bernskoetter, W. H.; Hazari, N.; Schneider, S. *J. Am. Chem. Soc.* **2014**, *136*, 10234−10237.
(29) Myers, T. W.; Berben, L. A. *Chem. Sci.* **2014**, *5*, 2771−2777.
(30) Gordon, J. C.; Kubas, G. J. *Organometallics* **2010**, *29*, 4682−4701.
(31) Kubas, G. J. *Chem. Rev.* **2007**, *107*, 4152−4205.
(32) Askevold, B.; Roesky, H. W.; Schneider, S. *ChemCatChem* **2012**, *4*, 307−320.
(33) Wang, N.; Wang, M.; Chen, L.; Sun, L. *Dalton Trans.* **2013**, *42*, 12059−12071.
(34) Rakowski DuBois, M.; DuBois, D. L. *Chem. Soc. Rev.* **2009**, *38*, 62−72.
(35) Liu, T.; DuBois, D. L.; Bullock, R. M. *Nat. Chem.* **2013**, *5*, 228−233.
(36) Bullock, R. M.; Appel, A. M.; Helm, M. L. *Chem. Commun.* **2014**, *50*, 3125−3143.
(37) Vogt, M.; Nerush, A.; Diskin-Posner, Y.; Ben-David, Y.; Milstein, D. *Chem. Sci.* **2014**, *5*, 2043−2051.
(38) Shima, S.; Pilak, O.; Vogt, S.; Schick, M.; Stagni, M. S.; Meyer-Klaucke, W.; Warkentin, E.; Thauer, R. K.; Ermler, U. *Science* **2008**, *321*, 572−575.
(39) Shima, S.; Ermler, U. *Eur. J. Inorg. Chem.* **2011**, *2011*, 963−972.
(40) Wang, W.-H.; Muckerman, J. T.; Fujita, E.; Himeda, Y. *New J. Chem.* **2013**, *37*, 1860−1866.
(41) Wang, W.-H.; Xu, S.; Manaka, Y.; Suna, Y.; Kambayashi, H.; Muckerman, J. T.; Fujita, E.; Himeda, Y. *ChemSusChem* **2014**, *7*, 1976−1983.
(42) Wang, W.-H.; Hull, J. F.; Muckerman, J. T.; Fujita, E.; Himeda, Y. *Energy Environ. Sci.* **2012**, *5*, 7923−7926.
(43) Wang, W.-H.; Muckerman, J. T.; Fujita, E.; Himeda, Y. *ACS Catal.* **2013**, *3*, 856−860.
(44) Sponholz, P.; Mellmann, D.; Junge, H.; Beller, M. *ChemSusChem* **2013**, *6*, 1172−1176.
(45) Neary, M. C.; Parkin, G. *Chem. Sci.* **2015**, *6*, 1859−1865.
(46) Fellay, C.; Yan, N.; Dyson, P. J.; Laurenczy, G. *Chem. - Eur. J.* **2009**, *15*, 3752−3760.
(47) Gan, W.; Snelders, D. J. M.; Dyson, P. J.; Laurenczy, G. *ChemCatChem* **2013**, *5*, 1126−1132.
(48) Gan, W.; Dyson, P. J.; Laurenczy, G. *ChemCatChem* **2013**, *5*, 3124−3130.
(49) Manaka, Y.; Wang, W.-H.; Suna, Y.; Kambayashi, H.; Muckerman, J. T.; Fujita, E.; Himeda, Y. *Catal. Sci. Technol.* **2014**, *4*, 34−37.
(50) Wang, W.-H.; Hull, J. F.; Muckerman, J. T.; Fujita, E.; Hirose, T.; Himeda, Y. *Chem. - Eur. J.* **2012**, *18*, 9397−9404.
(51) Oldenhof, S.; de Bruin, B.; Lutz, M.; Siegler, M. A.; Patureau, F. W.; van der Vlugt, J. I.; Reek, J. N. *Chem. - Eur. J.* **2013**, *19*, 11507−11511.

DOI: 10.1021/acscatal.5b01090
ACS Catal. 2015, 5, 5496−5504

(52) Fukuzumi, S.; Kobayashi, T.; Suenobu, T. *ChemSusChem* **2008**, *1*, 827−834.
(53) Himeda, Y.; Miyazawa, S.; Hirose, T. *ChemSusChem* **2011**, *4*, 487−493.
(54) Himeda, Y. *Green Chem.* **2009**, *11*, 2018−2022.
(55) Tanaka, R.; Yamashita, M.; Chung, L. W.; Morokuma, K.; Nozaki, K. *Organometallics* **2011**, *30*, 6742−6750.
(56) Dixon, H. B. F. *Biochem. J.* **1973**, *131*, 149−154.
(57) Zhao, Y.; Truhlar, D. *Theor. Chem. Acc.* **2008**, *120*, 215−241.
(58) Marenich, A. V.; Cramer, C. J.; Truhlar, D. G. *J. Phys. Chem. B* **2009**, *113*, 6378−6396.
(59) Oldenhof, S.; Lutz, M.; de Bruin, B.; Ivar van der Vlugt, J.; Reek, J. N. H. *Chem. Sci.* **2015**, *6*, 1027−1034.

DOI: 10.1021/acscatal.5b01090
ACS Catal. 2015, 5, 5496−5504